

AUTHOR QUERY FORM

	<p>Journal: J. Chem. Phys.</p> <p>Article Number: JCP23-AR-02018</p>	<p>Please provide your responses and any corrections by annotating this PDF and uploading it to AIP's eProof website as detailed in the Welcome email.</p>
---	--	--

Dear Author,

Below are the queries associated with your article. Please answer all of these queries before sending the proof back to AIP.

Article checklist: In order to ensure greater accuracy, please check the following and make all necessary corrections before returning your proof.

1. Is the title of your article accurate and spelled correctly?
2. Please check affiliations including spelling, completeness, and correct linking to authors.
3. Did you remember to include acknowledgment of funding, if required, and is it accurate?

Location in article	Query/Remark: click on the Q link to navigate to the appropriate spot in the proof. There, insert your comments as a PDF annotation.
Q1	Please check that the author names are in the proper order and spelled correctly. Also, please ensure that each author's given and surnames have been correctly identified (given names are highlighted in red and surnames appear in blue).
Q2	Please define SPC/E at first occurrence.
Q3	Please define PMEMD at first occurrence.
Q4	In the sentence beginning "By visually inspecting the eigenspectrum, the first few dominant modes...", please confirm that the term "result section" refers to Sec. I B.
Q5	Please confirm the change in author's initials in Ref. 1.
Q6	Please provide technical report number in Ref. 16.
	Please confirm ORCIDs are accurate. If you wish to add an ORCID for any author that does not have one, you may do so now. For more information on ORCID, see https://orcid.org/ .

Thank you for your assistance.

Jeremy D. Curuksu – 0000-0002-2077-9758

1 Spectral analysis of DNA superhelical dynamics 2 from molecular minicircle simulations

3 Cite as: J. Chem. Phys. 159, 000000 (2023); doi: 10.1063/5.0164440

4 Submitted: 22 June 2023 • Accepted: 22 August 2023 •

5 Published Online: 9 99 9999



■ Q1 Jeremy D. Curuksu^{a)}

6 AFFILIATIONS

7 Amazon.com, Inc., New York, New York 10001, USA and Center for Data Science, New York University,
8 New York, New York 10011, USA

9 ^{a)}Author to whom correspondence should be addressed: curukj@amazon.com

10 ABSTRACT

11 Torsional and bending deformations of DNA molecules often occur *in vivo* and are important for biological functions. DNA “under stress” is a conformational state, which is by far the most frequent state during DNA–protein and gene regulation. In DNA minicircles of length <100 base pairs, the combined effect of torsional and bending stresses can cause local unusual conformations, with certain base pair steps often absorbing most of the stress, leaving other steps close to their relaxed conformation. To better understand the superhelical dynamics of DNA under stress, molecular simulations of 94 bp minicircles with different torsional linking numbers were interpreted using Fourier analyses and principal component analyses. Sharp localized bends of nearly 90° in the helical axis were observed, which in turn decreased fluctuations of the rotational register and helped redistribute the torsional stress into writhe, i.e., superhelical turn up to 360°. In these kinked minicircles, only two-thirds of the DNA molecule bends and writhes and the remaining segment stays close to straight and preserves a conformational flexibility typical of canonical B-DNA (bending of 39° ± 17° distributed parsimoniously across 36 bp), which was confirmed and visualized by principal component analysis. These results confirm that stressed DNA molecules are highly heterogeneous along their sequence, with segments designed to locally store and release stress so that nearby segments can stay relaxed.

24 Published under an exclusive license by AIP Publishing. <https://doi.org/10.1063/5.0164440>

26 I. INTRODUCTION

27 The conformational flexibility of DNA fragments of length at or above 100 base pairs (bp) is often well described by a model
28 accounting only for linearly elastic deformations, but the combined
29 effect of torsional and bending stresses can cause local unusual
30 conformations.¹ Cyclization assays and atomic force microscopy
31 have both indicated that DNA bending energy alone is sufficient to
32 induce local unusual conformations in minicircles of length up to
33 85 bp² and when combined with torsional stress in minicircles up
34 to 339 bp.^{1,3}

35 Molecular dynamics (MD) simulations of DNA fragments
36 under torsional stress⁴ and bending stress (e.g., DNA minicircles
37 as in Refs. 1, 5, and 6) have suggested the spontaneous occurrence
38 of sharp localized twist and bent conformations. A 94 bp sequence
39 is often chosen because it imposes the typical level of curvature
40 observed in nucleosomal DNA *in vivo*, and it is also the length of
41 the DNA fragments that had the highest cyclization probability in
42 the experimental results that first indicated an unexpectedly high

43 flexibility of DNA on length scales shorter than its persistence
44 length.^{7,8} The occurrence of “kinked” conformations in DNA could
45 explain these experiments, and although such detailed conformations
46 cannot directly be observed using existing experimental technologies,
47 computer simulations give us an opportunity to describe in detail the different kinds of local conformations that most likely
48 occur in nature. DNA kinks have since been reported in many more
49 molecular simulations of DNA.^{1,3,9–11}

50 In this paper, the results of all-atom MD simulations for 94 bp
51 minicircles are interpreted using Fourier analyses and principal
52 component analyses. These minicircles have three different linking
53 numbers (underwound, relax, and overwound), different water
54 models (TIP3P¹² and SPC/E¹³), and different physiological
55 concentrations of ions with respect to minimal salt. The results help
56 understand the local conformations and the more global, superhelical
57 dynamics that characterize DNA under bending and torsional
58 stresses. Sharp localized bends of nearly 90° in the helical axis were
59 observed in the torsionally stressed minicircles but not in the torsionally
60 relaxed ones, in agreement with previous experimental and

theoretical studies.^{1,2} The DNA kinks observed in overwound minicircles are not associated with unusual DNA backbone substates but are strongly associated with the global minicircle structure and dynamics. These kinks decrease fluctuations of the rotational register and help redistribute the torsional stress into global superhelical turns (writhe). Most interestingly, only two-thirds of the minicircle structure bends and writhes and the remaining segment preserves a conformational flexibility typical of canonical B-DNA. This was measured and explicitly visualized by principal components analysis.

A. Material and methods

A circularized DNA fragment of 94 base pairs with three different values of torsional load and an otherwise regular superhelical structure was built using JUMNA (Junction Minimization of Nucleic Acids¹⁴) for the following sequence (as in Ref. 5): GGCCGGGTCG TAGCAAGCTC TAGCACCGCT TAAACG-CACG TACGCGCTGT CTACCGCGTT TTAACCGCCA ATAG-GATTAC TTACTAGTCT CTAC.

This is a closed, planar minicircle with a standard helical rise of 3.38 Å and a helical twist that was set to three different values, 30.6°, 34.5°, and 38.3°, respectively, corresponding to a linking number (Lk) of 8, 9, and 10. The linking number Lk is a mathematical invariant that describes the linking of closed curves in three-dimensional space and represents the number of times that two curves wind around each other, assuming no superhelical turn (writhe, see below). The two curves here are the two strands of the DNA double helix, and as long as there is no writhe such as in the initial structure built by JUMNA, the linking number is directly proportional to the cumulative inter-base pair twist. The linking numbers of 8, 9, and 10 correspond to underwound, relaxed, and overwound B-DNA conformations, respectively.

The superhelical dynamics can be measured by the time evolution of the writhe number Wr(t), which amounts to the wrapping of the double helix on itself and was obtained from White's formula,¹⁵

$$\text{Wr}(\text{t}) = \text{Lk} - \theta(\text{t}),$$

where Lk is the linking number, a fixed value for any given closed DNA molecule as long as no strand disruption accounts for their crossing, and $\theta(\text{t})$ is the twist number at time t obtained by computing the integral of the bp twist $\tau(s)$ along the minicircle contour line s ,

$$\theta = \frac{1}{2\pi} \int \tau(s) ds.$$

Note that a writhe number Wr of exactly "1" is equivalent to an amount of superhelical wrapping equal to 360°.

Each starting structure was refined by minimizing the total potential energy of the molecular system in JUMNA. A first triplet of systems (Lk = 8, 9, and 10) was created by adding an octahedral periodic box of explicit TIP3P water molecules¹² and potassium (K+) ions in a concentration sufficient to neutralize DNA phosphate negative charges (called "minimum salt" in the literature). Another triplet of systems (again Lk = 8, 9, and 10) was also created by replacing the TIP3P water model with SPC/E¹³ and adding an extra 150 mM of potassium chloride (KCl), i.e., 140 K+ and 140 Cl- ("physiological conditions"). Other water and salt setups

were explored, too, such as minimal salt combined with the SPC/E water model. Molecular dynamics simulations were all performed with the AMBER 10 suite of programs (PMEMD module¹⁶) and the parm-bsc0 force field.⁵ Each system was equilibrated by a series of energy minimizations and short MD runs (<1 ns). The production runs consisted of 100 ns unrestrained MD simulations in an NPT ensemble (see Ref. 1 for more context).

The analysis of the MD trajectories contains two parts, corresponding to an examination at the bp level and then a follow-up of the dynamics in terms of global shape, i.e., the superhelical dynamics. Conformational frames along the trajectories were saved every 1 ps and analyzed with CURVES+¹⁷ to obtain both helical parameter and backbone torsion angle time series. CURVES+ was also used to compute the overall bend angle imposed by the kinks that emerged in the simulations (sharp localized bend in the superhelix), by calculating two linear axes for the 10 bp segments preceding and following the observed kink and computing the angle between these axes.

We further characterized the global shape of DNA minicircles using spectral analyses. First, the time evolution of the rotational register was obtained by a Fourier analysis of the helical roll angle distribution along the DNA sequence.¹⁸ This is a harmonic decomposition in space, not in time: in each conformational frame, a Fourier analysis in polar coordinates (also called the *amplitude-phase* form of a Fourier series) can decompose the 94 bp signal into 48 scaled cosine functions (i.e., 94/2 + 1), each with an amplitude and a phase shift,

$$\omega(\hat{s}) = a_0 + \sum_{n=1}^{47} a_n \cos(2\pi n \hat{s} - \varphi_n),$$

where \hat{s} represents a discretized version of the minicircle contour line s (94 steps), $\omega(\hat{s})$ is the (discretized) bp roll along \hat{s} , a_n is the amplitude of the n th harmonic, φ_n is the phase shift of the n th harmonic, and a_0 is the mean value of $\omega(\hat{s})$, often called the zeroth harmonic. The number n corresponds to the number of cycles each sinusoid makes over the length of the minicircle sequence (94 steps). In a planar B-DNA minicircle, the sinusoid for which n equals the value of the linking number Lk will have much higher amplitude than others because it physically represents the number of complete 360° turns the DNA double helix makes along the minicircle sequence, and there is, indeed, exactly n helical turns in a planar B-DNA minicircle with Lk = n . For example, in SKC10, the sinusoid of the highest amplitude corresponds to a sharp peak in the frequency domain [Fig. 5(a)] and its bandwidth is equal to the linking number [Fig. 5(b)]. Its bandwidth ($n = 10$) corresponds to the number of complete helical turns of 360° made over the length of the minicircle sequence. This dominant harmonic represents a function filtered from noise (local fluctuations at the bp level) that describes the periodic curvature along the double helix, assuming maxima and minima point toward the center of a planar minicircle. As also discussed in Ref. 5, the phase parameter of this function accounts for rotation of the double helix around its own superhelical axis, called the *rotational register*. More details on the rotational register in the context of circularized DNA can be found in Refs. 5 and 19.

Finally, a principal component analysis (PCA) of the conformational fluctuations in the Cartesian coordinates of non-hydrogen atoms was carried out. Given that DNA bases are nearly planar and modeled mostly as rigid bodies in MD simulations, they typically do not show significant fluctuations compared with fluctuations

“between” bases. Each has six degrees of freedom (three translations and three rotations); thus, in total, the PCA has a dimension of $94 \times 2 \times 6 = 1128$ significant degrees of freedom. The projection was made on the first 50 eigenvectors to analyze whether there were global superhelical concerted motions. Two separate PCAs were carried out, one on the phase of the trajectories prior to kink events occurred and one on the following phase where DNA molecules contain kinks (as mentioned above, kinks are sharp localized bends in the superhelix). For each phase, the corresponding trajectory was projected onto the first 50 eigenvectors within the PTRAJ module of AMBER 10.¹⁶ By visually inspecting the eigenspectrum, the first few dominant modes were selected: the eigenspectrum showed that the first 3–4 vectors had much higher magnitude than all subsequent eigenvectors; hence, a projection on the first five eigenvectors was chosen to ensure that no dominant mode would be ignored when interpreting the characteristic superhelical shapes presented in the result Sec. I B. Interactive Essential Dynamics software²⁰ was used to visualize conformational frames along these modes and characterize the global shape of minicircles when kinks occur.

■ Q4

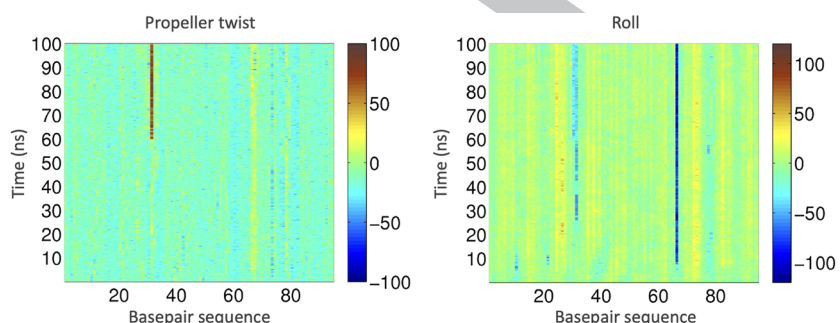


FIG. 1. Time evolution of bp propeller (left) and roll (right) in the overwound minicircle ($Lk = 10$) simulated with the SPC/E water model and 150 mM KCl. Base pairs (for propeller) and base pair steps (for roll) are numbered from left to right along the horizontal axis. Simulation time increases upward along the vertical axis. The color bar indicates the angular value in degrees.

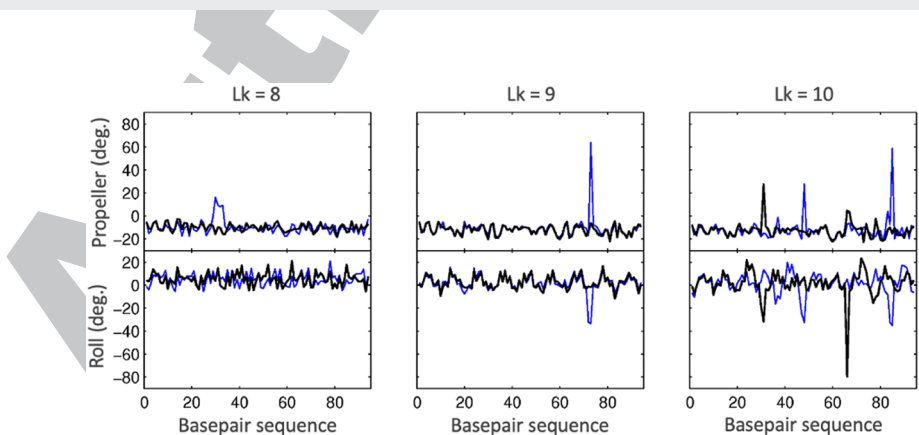


FIG. 2. Average bp propeller (up) and roll (down) in the underwound (left), relaxed (middle), and overwound (right) minicircles. Black: Simulation with the SPC/E water model and 150 mM KCl. Blue: Simulation with the TIP3P water model and minimal salt. As noted in the text, the increased propeller observed in the underwound minicircle (blue curve) is not due to kinking but local unwinding.

B. Results

1. Overwound DNA minicircles

In this section, we describe two MD trajectories of 94 bp minicircle with $Lk = 10$. At the equivalent torsional stress in Ref. 5, two types of kinks occurred at two different positions in the minicircle. In type I kink, a single bp step completely unstacks, leading to a roll value of the order of 90° , with little disturbance of the neighborhood. In type II kink, three successive bp are involved, and the Watson-Crick hydrogen bonding of the central bp is broken such that each base stacks on its 5' neighbor.

The minicircle simulation called TK10 corresponds to minimal salt (K⁺ counterions) with the TIP3P water model, and the one called SKC10 is a simulation with 150 mM KCl and the SPC/E water model (Fig. 1). Both TK10 and SKC10 evolve toward a characteristic shape referred to as a Swiss-roll in Ref. 5, where a close-to-straight segment of ~36 bp is capped at either end with kinks and joined to the remaining highly writhed S-shaped segment. A noticeable difference is that although two type II kinks are observed in TK10, type I and type II kinks are observed in SKC10 (Fig. 2).

219
220

221

222

223

224

225

226

227

228

229

230

231

232

233

234

TABLE I. Conformational deformations observed in each simulation.

Simulate ^a	Base pair step index	Base pair step	Start-end (ns)	Type of deformation	Bend angle ^b (deg)
SKC10	66	CG	10–100	Type I kink	108(9)
	30/31	TTA	60–100	Type II kink	109(15)
TK10	47/48	CTG	40–100	Type II kink	101(14)
	84/85	TAG	5–100	Type II kink	101(8)
SKC9				N/A	
SK9				N/A	
TK9	72/73	TAG	15–100	Type II kink	73(11)
SKC8	14	CA	65–100	Unwound step	45(12)
TK8	30	AA	5–100	Unwound step	54(12)
	32	AA	10–100	Unwound step	47(14)

^aThe name convention refers to minicircles described in the text.^bThe average bend angle and its standard deviation (in parentheses) were calculated between the adjacent 10 bp segments following and preceding the kink and over the time window indicated in column 4.

235 The type I kink in SKC10 appears at a CG bp step early in the
 236 simulation (10 ns, see Table I) and closely resembles that originally
 237 described in 1975 by Crick and Klug²¹ with a roll angle close to 90°
 238 directed toward the local minor groove.

239 **2. Torsionally relaxed DNA minicircles**

240 Three trajectories for Lk = 9 corresponding to the absence of
 241 torsional stress were produced for the 94 bp minicircle. The simulate
 242 referred to as TK9 (TIP3P, minimal salt) evolves toward a teardrop
 243 shape with a single type II kink early in the simulation. In contrast,
 244 both simulates with SPC/E, which are SKC9 (150 mM KCl) and SK9
 245 (minimal salt), remain un-kinked (i.e., the curvature of the DNA
 246 molecule is parsimoniously distributed along its sequence) over the
 247 entire course of the simulations (Fig. 2). The results for Lk = 9 are
 248 thus in line with what was simulated in Ref. 5 and later in Ref. 19,
 249 and also with cyclization experiments:² kinks are not needed to deal
 250 with the bending load typically observed in nucleosomal DNA if it is
 251 torsionally relaxed.

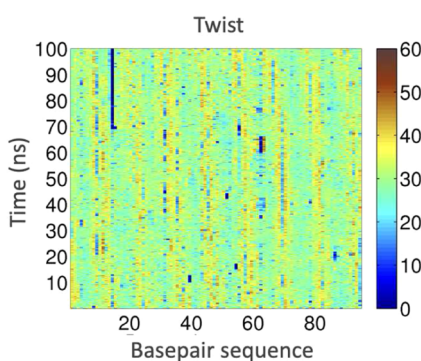
252 We also carried out simulations with the same solvent conditions
 253 as in SKC9 but with a sequence truncated at 89 and 99 bp and
 254 with Lk = 9. The goal was to impose a torsional stress intermediary
 255 between Lk = 9 and Lk = 10 and between Lk = 8 and Lk = 9,
 256 respectively. In these simulates, we did not observe any kink formation
 257 either, not even temporarily, which supports the assertion made
 258 above.

259 **3. Underwound DNA minicircles**

260 We carried out MD simulations of underwound minicircles,
 261 which were not inquired in Ref. 5. The same naming convention
 262 as above is used in this section, where TK8 refers to minicircle
 263 simulations with a TIP3P water model and minimal salt (K+ counterions),
 264 and SKC8 refers to minicircle simulations with a SPC/E water model
 265 and a physiological (150 mM) KCl salt concentration.
 266 No kink was observed, but the negative torsion stress in TK8 and
 267 SKC8 was locally absorbed by one bp step (SKC8, Fig. 3) or two bp
 268 steps (TK8), respectively, CA and twice AA steps (Table I), in
 269 complete agreement with.⁴ As can be seen in Fig. 3, local hotspots of
 270 unwound bp step first emerge transiently at diverse positions along

271 the sequence, and in a second phase of the simulation, the CA step
 272 at position 14 completely unwinds (from 70 ns up to the end of the
 273 simulation). These local unwindings are coupled to a significant
 274 change in the propeller in the case of TK8 (Fig. 2), but no other sig-
 275 nificant change in the helical parameter is observed (e.g., bending
 276 or opening). Hence, these hotspots help in relieving the global tor-
 277 sional stress,⁴ but neither kink nor base pair opening appears needed
 278 to deal with this bending and torsional load.

279 The lifetime of individual hydrogen bonds in each bp is cor-
 280 related with the unwinding events described above. For example,
 281 in the TK8 simulation, the average lifetime of broken hydrogen
 282 bonds is 3.3 fs, with two peaks in the distribution of average lifetime
 283 along the sequence corresponding to 27.3 and 26.0 ps, respectively,
 284 located where two bp steps are unwound. In the SKC8 simula-
 285 tion, where only one bp step is unwound, the maximum lifetime
 286 of broken hydrogen bonds, 12.5 ps, also happens where unwind-
 287 ing happened. However, with the combined effect of the transient
 288 unwinding events that occur during the first 70 ns, the maximum



288
 289 **FIG. 3.** Time evolution of bp twist in the underwound minicircle (Lk = 8) simulated
 290 with the SPC/E water model and 150 mM KCl. The same legends as in Fig. 1.
 291 Note that one vertical stripe corresponding to a complete unwinding of one bp step
 292 is observed, whereas in the simulation with TIP3P and minimal salt (not shown),
 293 two vertical stripes were observed.

293 lifetime averaged over the sequence in SKC8 is 0.15 ps, then drops
 294 down to only 0.02 ps in the last 30 ns of the trajectory when the
 295 CA step at position 14 steadily unwinds and transient unwinding
 296 stops. Thus, the transient unwinding events correlate with a strands,
 297 and above 85% when ~10-fold increase in the maximum lifetime of
 298 broken hydrogen bonds.

299 4. Conformational substates of DNA backbone

300 Non-canonical DNA backbone substates were more frequent in
 301 the unwound and kinked bp steps than in standard B-form DNA. In
 302 the unwound bp steps, several backbone dihedrals ($\alpha, \gamma, \varepsilon, \zeta, \xi$) can
 303 be found in some non-canonical conformations, but with no clearly
 304 preferred substate.

305 In the kinked bp steps, a preference toward the non-canonical
 306 substate of ε/ζ called BII is observed on at least one of the strands at
 307 the position of the kink and also in its neighborhood. The population
 308 of BII substates over all ε/ζ instances is less than 15% of the total
 309 trajectories on average, see Table II. However, it is increased to 79%
 310 on strand 1 and 25% on strand 2 where type I kink occurs (step 66)
 311 in the SKC10 simulation, and 47% and 70% at the neighboring step
 312 67 (then, it drops back to <15%), respectively. This is even clearer
 313 considering all non-canonical substates, i.e., not only BII: 90%/66%
 314 at step 66 and 93%/88% at step 67, respectively. For the type II kinks,
 315 the population of BII conformations is systematically above 50% on
 316 both strands and above 85% when considering all non-canonical ε/ζ
 317 substates, respectively.

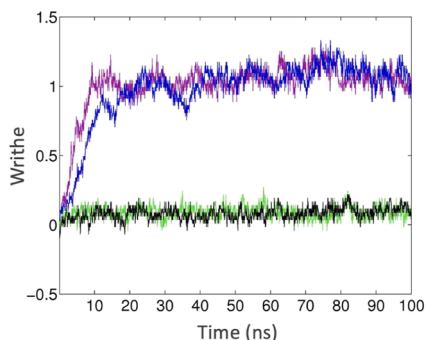
318 Transitions in α/γ DNA backbone dihedrals are less pro-
 319 nounced. In the neighborhood of kinks, the average population of
 320 $\gamma/g+$ substates is between 5% and 10%, whereas it is 1%–3% when
 321 averaged over all α/γ instances (Table II).

322 Apart from where kinks and unwound steps occur (as dis-
 323 cussed above), the distribution of backbone dihedral substates is very
 324 similar between all current simulations (Table II).

325 5. DNA superhelical dynamics

326 In this section, the DNA superhelical dynamics is interpreted in
 327 terms of writhe, rotational register derived from a Fourier analysis,
 328 and molecular projections on dominant eigenvectors derived from a
 329 principal component analysis.

330 The dynamics of the DNA minicircles can be interpreted in
 331 terms of their global shapes by measuring the time evolution of
 332 the writhe number defined by the White formula in the Methods



347 FIG. 4. Time evolution of writhe Wr in the overwound and underwound minicircle
 348 simulations. Black: SKC8, Green: TK8, Blue: SKC10, Magenta: TK10.

349 section. A key takeaway from this paper is that all overwound mini-
 350 circles ($L_k = 10$) transform the totality of excess twist into an equal
 351 amount of writhe. In contrast, underwound minicircles stay planar
 352 (Fig. 4). A relationship between DNA writhing and the occurrence
 353 of kink was apparent: the first kink event emerges at 10 ns for SKC10
 354 (Fig. 1) and 5 ns for TK10, and in each case, this point in time coin-
 355 cides with when the progressive build up of writhe up to 360° , i.e.,
 356 $Wr = 1$, is complete. In other words, DNA kinks when $Wr = 1$. This
 357 was observed in all simulations carried out here.

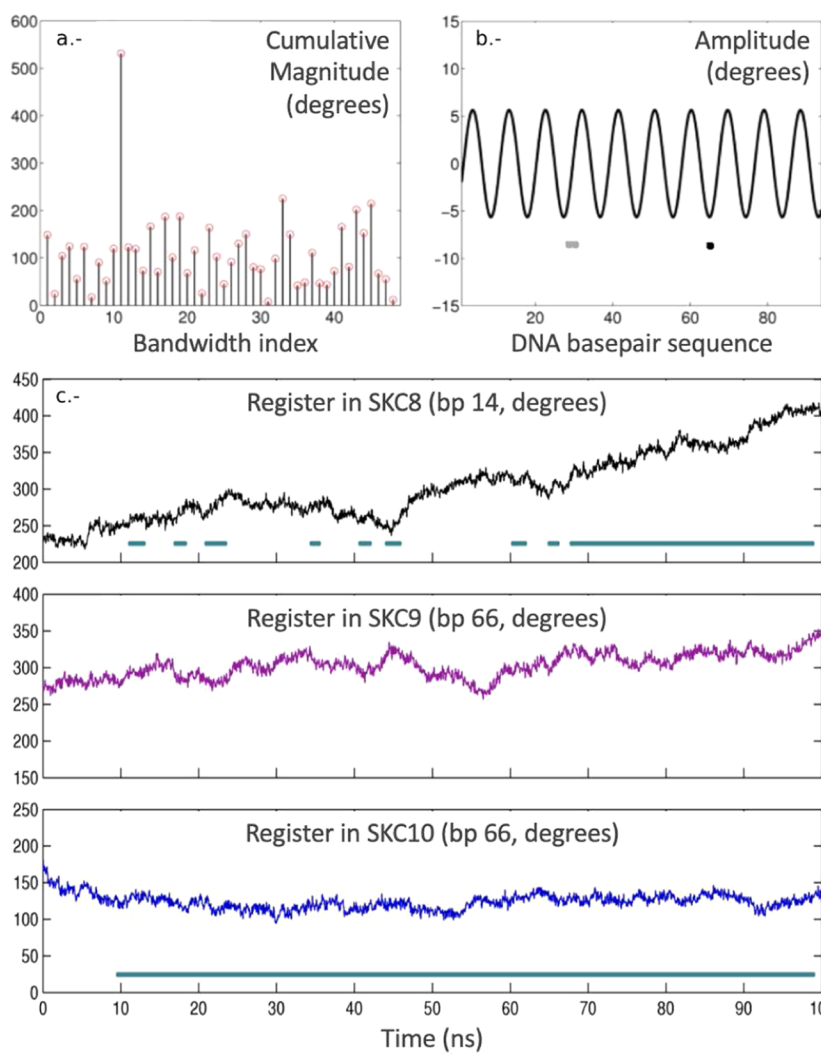
358 The superhelical dynamics of DNA minicircles can be further
 359 interpreted by measuring the time evolution of rotational register
 360 obtained from a Fourier analysis in polar coordinates of the roll fluc-
 361 tuation along the minicircle, as described in the Methods section.
 362 The occurrence of bp kink has been proposed to lock the rotational
 363 register into a small range of values,⁵ which could be beneficial *in*
 364 *vivo* by preventing arbitrary rotations of DNA molecules during
 365 protein-DNA recognition. This was also observed in the current
 366 simulations [Fig. 5(c)]. For SKC10, the register stabilizes around a
 367 mean value of 118.1° (standard deviation = 8.9°) after the first kink
 368 occurs at 10 ns (Fig. 1) and even more clearly after 60 ns when the
 369 second kink occurs (mean = 127.5° , standard deviation = 5.8°). This
 370 superhelical configuration corresponds to the minor groove of the
 371 kinked step facing inward toward the center of the minicircle. Inter-
 372 estingly, the register value at the start of the simulation was 180.8° ,
 373 which placed the minor groove of the step that kinks (step 66, Fig. 1)
 374 exactly inward toward the center of the minicircle [Fig. 5(b)].

375 When the kinks occur, the frequency domain of the Fourier
 376 analysis is doubly peaked, meaning two cosine functions are
 377 most prevalent when reconstituting the original roll distribution.
 378 Figure 5(b) shows that both kinks are located at positions of max-
 379 imum bending toward the center of the minicircle *before* writhe
 380 builds up (during the first 10 ns, Fig. 4). In these first few ns, when
 381 kinks have not happened yet, the un-kinked minicircle has a mostly
 382 planar superhelix, and the frequency domain remains single-peaked
 383 [Fig. 5(a)]. Indeed, Fig. 5(a) shows that the sinusoid corresponding
 384 to $n = 10$ is early in the simulation ($t = 5$ ns), the most dominant
 385 frequency by far, and Fig. 5(b) shows the exact distribution of this
 386 dominant sinusoid along the DNA base pair sequence together with
 387 the exact position of the two kinks, respectively, of type II (gray dots)
 388 and type I (black dot). In Fig. 5(b), it can be seen that these dots are

333 TABLE II. Average proportions of DNA backbone substates.

334 Simulate ^a	335 α/γ g-/g+	336 α/γ others	337 ε/ζ BI	338 ε/ζ BII	339 ε/ζ others
SKC10	0.98	0.02	0.79	0.14	0.07
TK10	0.98	0.02	0.80	0.14	0.06
SKC9	0.99	0.01	0.76	0.17	0.07
SK9	0.99	0.01	0.83	0.12	0.05
TK9	0.99	0.01	0.80	0.13	0.07
SKC8	0.98	0.02	0.88	0.09	0.03
TK8	0.97	0.03	0.87	0.08	0.05

345 ^aThe name convention refers to minicircles described in the text.



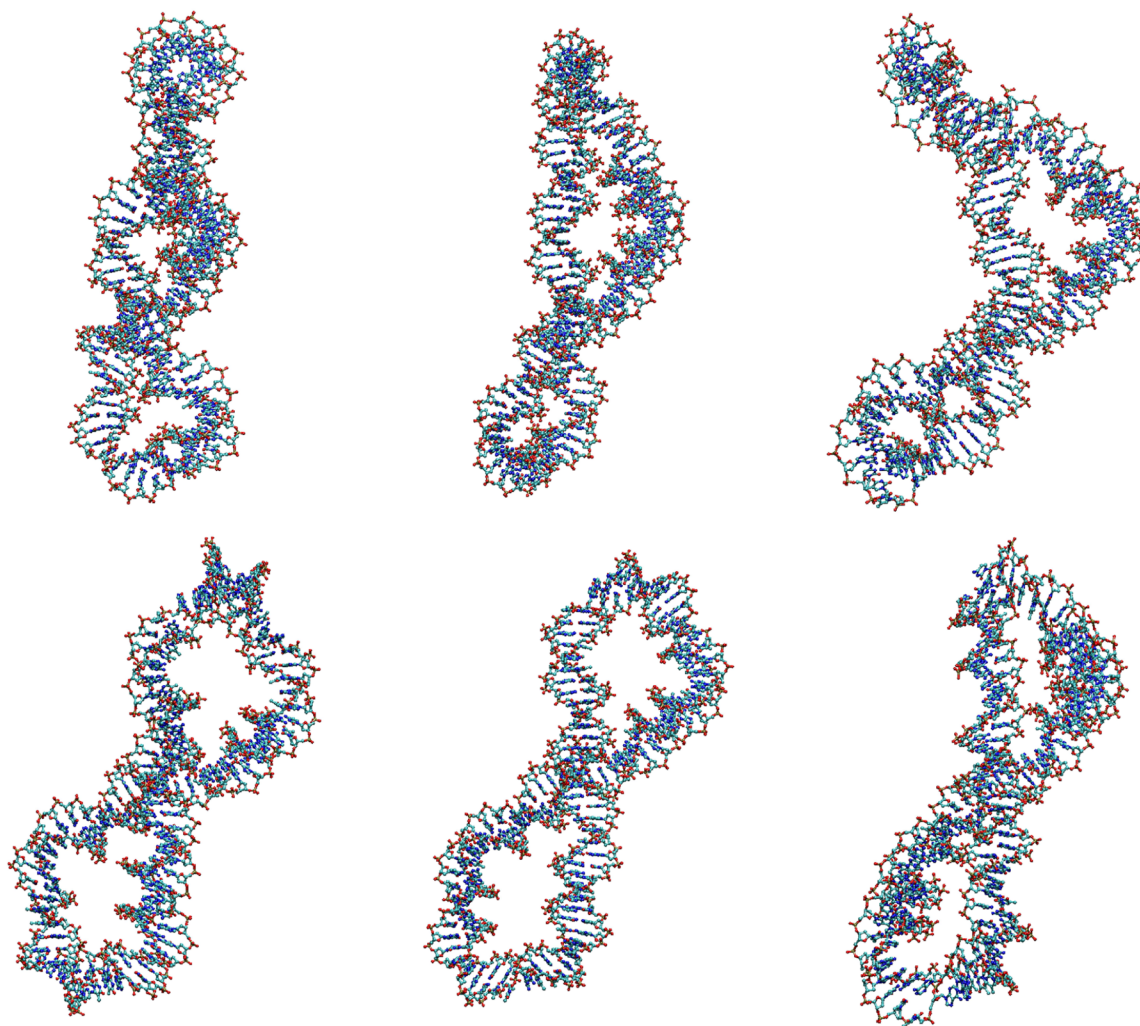
389 **FIG. 5.** Fourier series analysis. (a) Frequency domain obtained via discrete Fourier transform in polar coordinates of the bp roll distribution in SKC10 at time $t = 5$ ns. Note
390 that the cosine function corresponding to the first bandwidth index is a constant equal to the average value of roll along the DNA sequence, which shifts all bandwidth indices
391 by +1. (b) Scaled cosine function corresponding to the 11th bandwidth index in the frequency domain of SKC10 at time $t = 5$ ns. Positions of kink type II (gray dots) and type
392 I (black dot) are indicated. (c) Phase of the 9th (black), 10th (red), and 11th (blue) scaled cosine function against time for SKC8, SKC9, and SKC10, respectively, which is
393 an approximation to the relative change in rotational register. The phase (in absolute value) was measured at the bp step position indicated on the y-axis. The lines in cyan
394 indicate the time-lines of transient unwinding in SKC8 and of kinking in SKC10.

395 precisely located at the apex of some peaks (i.e., maximum bending)
396 in this dominant sinusoid.

397 In the relaxed (SKC8) or underwound (SKC9) minicircle simulations,
398 which do not induce any kink, the rotational register drifts
399 more loosely over time with a difference of $\sim 180^\circ$ between the
400 beginning and the end of the simulation in SKC8 (mean value
401 = 304.1° , standard deviation = 48.6°). The “flickering” movement
402 of the unwound steps described earlier could explain why the reg-
403 ister changes rapidly in the underwound minicircles. Figure 5(c)
404 shows that the transient unwinding of bp steps is correlated with
405 some sudden changes in the rotational register. For example, some

406 sudden increases in the register are observed at 20, 25, 45, and 65 ns
407 in Fig. 5(c), and these correspond to the exact timelines of spots
408 observed in Fig. 3, respectively, at positions 54, 86, 31, and 31. When
409 a CA step at position 14 unwinds and remains unwound in the final
410 30 ns of the simulation, the register continuously rotates by $\sim 120^\circ$ in
411 total across these final 30 ns.

412 Finally, a principal component analysis of the kinked minicircles
413 was used to characterize their superhelical dynamics in terms of
414 average conformation and maximum displacements away from this
415 average conformation (Fig. 6). When projecting the DNA molecule
416 from its original Cartesian coordinates onto its first five eigenvectors
417



422 **FIG. 6.** PCA of the section of the trajectory where kinking occurs in the SKC10 simulation (from 10 to 100 ns). The conformational frames are projections along the first five
423 eigenvectors. The first and second rows are alternative views of an identical structure after rotation by 90° about the vertical. The middle frame corresponds to the average
424 coordinates. Left/right frames correspond to maximum displacement, respectively, below and above the average coordinates on the first five eigenvectors.

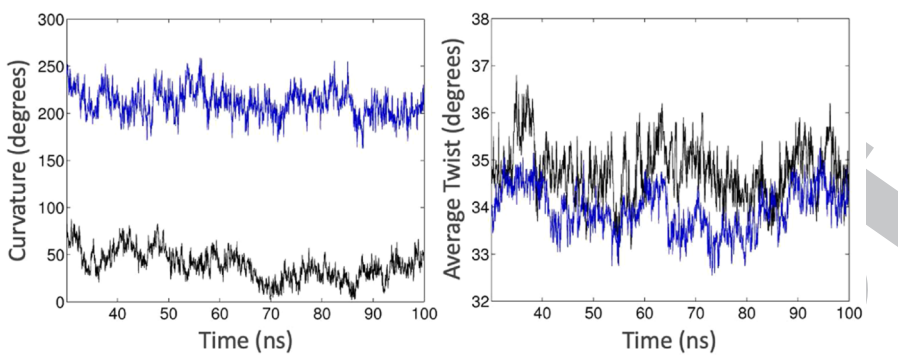
425 in the SKC10 trajectory (after kinks occur, i.e., final 90 ns, Fig. 6),
426 the Swiss-roll shape described above corresponds to the average
427 conformation (middle frame in Fig. 6). That is a close-to-straight
428 segment of ~36 bp joined to a highly writhed S-shaped segment.
429 At the maximum displacement in either direction onto the first five
430 eigenvectors, the observed shapes resemble what one would obtain,
431 respectively, from pulling (left-hand side in Fig. 6) and pushing
432 (right-hand side in Fig. 6) the two ends of an *arrow-bow*.

433 In the characteristic shape obtained by maximum displacement
434 below the average conformation, the overall writhe increases: the
435 long and small segments both wrap around each other (Fig. 6, left),
436 whereas in the average shape, the small segment is straight (Fig. 6,
437 middle). In the analogy of the arrow-bow, this corresponds to the
438 string wrapping around the limb when pulling because the string
439 cannot stretch further, which is also expected in DNA because it is

443 energetically easier to rotate an originally straight DNA superhelix
444 than to stretch it.

445 In the characteristic shape obtained by maximum displacement
446 above the average conformation, a significant bending is observed
447 for both the long and the small segments, with the latter swept along
448 on the concave side of the long segment (Fig. 6, right). In the analogy
449 of the arrow-bow, this corresponds to the string curving parallel to
450 the limb when compressing it. As the two ends are pushed inward,
451 the net distance between the two ends decreases.

452 The average curvature of the writhed segment is 211.2° when
453 excluding a segment of 10 bp surrounding each kink, and the cur-
454 vature of the straight segment is 39.3° (Fig. 7). Their standard
455 deviations are similar, that is, 15.4° and 17.0°, respectively. The bp
456 twist value in the two segments varies between 20° and 40° on dif-
457 ferent bp steps (not shown) without clear bp specificity from one



458
459
460 **FIG. 7.** Curvature and sequence-averaged bp twist in the short segment (black) and long segment (blue) of the Swiss-roll shape, i.e., for the section of the trajectory where
461 two kinks are present (from 30 to 100 ns) in the SKC10 simulation. The DNA segments going from bp 35–61 (short segment) and the segment composed of bp 1–25 + bp
462 71–94 (long segment) were analyzed independently. These were selected to exclude 5 bp on both sides of each kink.
463
464

465 time frame to the next. However, on average, the bp steps in the
466 writhed segment have a lower twist of 33.9° compared with 34.8°
467 in the straight segment (Fig. 7). The average twist fluctuation is
468 similar in the short and long segments, with standard deviations of 0.6°
469 and 0.5° , respectively. These results confirm that the short segment
470 of 36 bp preserves a conformational flexibility typical of canonical
471 B-DNA. Thus, the sharp localized bends flanking this small seg-
472 ment can be interpreted as a mechanism to locally store and release
473 stress so that the 36 bp segment can stay relaxed. The slight writhing
474 and bending of this segment observed in the most extreme devia-
475 tions during the PCA is typical of B-DNA and thus supports the
476 hypothesis that the superhelical dynamics of nucleosomal DNA can
477 be tightly controlled and can play a key role in gene regulation.^{1,4}

478 II. CONCLUSION

479 All-atom simulations of 94 bp DNA-circularized molecules
480 under the influence of torsional stress were analyzed, and the super-
481 helical dynamics was interpreted using Fourier analyses and
482 principal component analyses. Simulations were repeated with different
483 water models and salt concentrations. Every simulation of the over-
484 wound minicircles leads to sharp localized bends in the helical axis
485 (kinks). Simulations of the relaxed and underwound minicircles did
486 not generally lead to kinks in the helical structure but led to some
487 localized unwinding of base pair steps steadily or transiently. The
488 “flickering” movement of the unwound steps can explain why the
489 rotational register changes more rapidly in underwound DNA. This
490 could be biologically important in making it easier for DNA loops to
491 rotate to bring specific interaction sites into contact.

492 In the overwound minicircles, kinks are localized at positions
493 of high curvature in the overall superhelical shape of the minicir-
494 cle and suppress fluctuations in the rotational register. They do
495 not seem associated with unusual transitions in the DNA backbone
dihedral angles, except for a larger proportion of the so-called BII
 ε/ζ state. Because the excess twist is almost entirely transformed
into writhe by the time the first kinks occur, it is tempting to pro-
pose that the build up of writhe causes the formation of kinks in
DNA.

496 Although the underwound minicircles transform the global
497 deficit in twist into local hotspots of fully unwound base pair steps,
498 the overwound minicircles transform the excess twist (all of it) into
499 writhing and give rise to a characteristic shape called Swiss-roll,
500 similar to an arrow-bow: a relatively straight segment of 36 bp at each
501 end of which a kink occurs and joined by a highly writhed longer
502 segment. The superhelical dynamics of the kinked, overwound DNA
503 can be summarized as going from superhelical wrapping to superhe-
504 lical bending, i.e., a concerted hinge motion that involves bending
505 the small segment instead of twisting it. In both cases, the range
506 of bending ($39^\circ \pm 17^\circ$ for 36 base pair steps) and twisting (34.8°
507 $\pm 0.6^\circ$ per base pair step) in the small segment remains within the
508 canonical B-DNA range, even during the maximum displacements
509 observed along the principal components of the conformational
510 eigenspectrum.

511 These results confirm that stressed DNA molecules are highly
512 heterogeneous along their sequence, with segments designed to
513 locally store and release stress so that nearby segments can stay
514 relaxed. This supports the hypothesis that the superhelical dynam-
515 ics of nucleosomal DNA can be tightly controlled and thus can play
516 a key role in gene regulation. For example, when some DNA is repli-
517 cated or transcribed *in vivo*, a multi-partner complex must form
518 before a polymerase can enter its active state, and the DNA helix
519 undergoes a 180° loop around the activation complex.^{22,23} In addi-
520 tion, in many cases of DNA-protein interactions, the binding site
521 must bend and twist to facilitate the positioning of specific chem-
522 ical groups on the protein along the DNA molecule.^{24,25} Although
523 these requirements have been studied in isolation, in most eukary-
524 otes and prokaryotes, the *in vivo* state of DNA molecules is sharply
525 bent and twisted around nucleosomal particles: each human cell
526 contains ~ 2 m of DNA if stretched end-to-end; however, the nucleus
527 of a human cell is only about $6\ \mu\text{m}$ in diameter. Thus, DNA flexibil-
528 ity plays a role not only in the compaction but also in “permitting
529 access” to the genetic material by allowing for transient unwrapping
530 needed for gene expression. The local DNA deformations identified
531 in this paper, such as base pair unwinding and kinks, could explain
532 how DNA interacts with proteins under such stress because in most
533 protein-DNA interactions, DNA bending and twisting angles are
534 relatively small (angular values are typical of “canonical” B-DNA
535

conformations) and must have precise, sequence-dependent values for the interaction to take place. DNA base pair unwinding and kinks could regulate the global superhelical dynamic of DNA molecules in at least two ways, by (1) allowing more or less rotation of the double helix on itself to bring specific interaction sites into contact and (2) locally absorbing stress so that nearby segments can stay relaxed in a canonical B-DNA conformation.

Finally, the local DNA deformations identified in this paper happen at sequence steps in agreement with what the theory and experiment would suggest.^{10,26} For example, DNA kinks are observed at Py/Pu and Py/Py/Pu steps, but never inside an A-tract. As a follow-up study, we will look at minicircles with shorter lengths and specific sequences such as the ones proposed in Refs. 4 and 26 to assess more systematically the extremes of DNA rigidity as a function of its sequence.

ACKNOWLEDGMENTS

The author thanks Richard Lavery, Krystyna Zakrzewska, and John Maddocks for their suggestions, advice, and encouragement during this research.

AUTHOR DECLARATIONS

Conflict of Interest

The author has no conflicts to disclose.

Author Contributions

Jeremy D. Curuksu: Conceptualization (equal); Formal analysis (equal); Methodology (equal); Visualization (equal); Writing – original draft (equal); Writing – review & editing (equal).

DATA AVAILABILITY

The data that support the findings of this study, including demos of the PCA superhelical dynamics, are available from the corresponding author upon reasonable request.

REFERENCES

- ¹A. L. B. Pyne, A. Noy, K. H. S. Main, V. Velasco-Berrelleza, M. M. Piperakis, L. A. Mitchenall, F. M. Cugliandolo, J. G. Beton, C. E. M. Stevenson, B. W. Hoogenboom *et al.*, “Base-pair resolution analysis of the effect of supercoiling on DNA flexibility and major groove recognition by triplex-forming oligonucleotides,” *Nat. Commun.* **12**, 1053 (2021).
- ²Q. Du, A. Kotlyar, and A. Vologodskii, “Kinking the double helix by bending deformation,” *Nucleic Acids Res.* **36**, 1120–1128 (2007).
- ³Q. Wang, R. N. Irobalieva, W. Chiu, M. F. Schmid, J. M. Fogg, L. Zechiedrich, and B. M. Pettitt, “Influence of DNA sequence on the structure of minicircles under torsional stress,” *Nucleic Acids Res.* **45**, 7633–7642 (2017).
- ⁴A. Reymer, K. Zakrzewska, and R. Lavery, “Sequence-dependent response of DNA to torsional stress: A potential biological regulation mechanism,” *Nucleic Acids Res.* **46**, 1684–1694 (2018).
- ⁵F. Lankas, R. Lavery, and J. H. Maddocks, “Kinking occurs during molecular dynamics simulations of small DNA minicircles,” *Structure* **14**, 1527–1534 (2006).
- ⁶L. J. Maher, “DNA kinks available . . . if needed,” *Structure* **14**, 1479–1480 (2006).
- ⁷T. E. Cloutier and J. Widom, “Spontaneous sharp bending of double-stranded DNA,” *Mol. Cell* **14**, 355–362 (2004).
- ⁸P. A. Wiggins, T. van der Heijden, F. Moreno-Herrero, A. Spakowitz, R. Phillips, J. Widom, C. Dekker, and P. C. Nelson, “High flexibility of DNA on short length scales probed by atomic force microscopy,” *Nat. Nanotechnol.* **1**, 137–141 (2006).
- ⁹S. A. Harris, C. A. Laughton, and T. B. Liverpool, “Mapping the phase diagram of the writhe of DNA nanocircles using atomistic molecular dynamics simulations,” *Nucleic Acids Res.* **36**, 21–29 (2007).
- ¹⁰J. Curuksu, M. Zacharias, R. Lavery, and K. Zakrzewska, “Local and global effects of strong DNA bending induced during molecular dynamics simulations,” *Nucleic Acids Res.* **37**, 3766–3773 (2009).
- ¹¹J. S. Mitchell, C. A. Laughton, and S. A. Harris, “Atomistic simulations reveal bubbles, kinks and wrinkles in supercoiled DNA,” *Nucleic Acids Res.* **39**, 3928–3938 (2011).
- ¹²W. L. Jorgensen, J. Chandrasekhar, J. D. Madura, R. W. Impey, and M. L. Klein, “Comparison of simple potential functions for simulating liquid water,” *J. Chem. Phys.* **79**, 926–935 (1983).
- ¹³H. J. C. Berendsen, J. R. Grigera, and T. P. Straatsma, “The missing term in effective pair potentials,” *J. Phys. Chem.* **91**, 6269–6271 (1987).
- ¹⁴R. Lavery, K. Zakrzewska, and H. Sklenar, “JUMNA (junction minimisation of nucleic acids),” *Comput. Phys. Commun.* **91**, 135–158 (1995).
- ¹⁵J. H. White, “Self-linking and the Gauss integral in higher dimensions,” *Am. J. Math.* **91**, 693 (1969).
- ¹⁶D. A. Case, T. A. Darden, T. E. Cheatham, C. L. Simmerling, J. Wang, R. E. Duke, R. Luo, M. Crowley, R. C. Walker, W. Zhang *et al.*, Amber 10, Technical Report No. ■, University of California, 2008.
- ¹⁷R. Lavery, M. Moakher, J. H. Maddocks, D. Petkeviciute, and K. Zakrzewska, “Conformational analysis of nucleic acids revisited: Curves+,” *Nucleic Acids Res.* **37**, 5917–5929 (2009).
- ¹⁸T. C. Bishop, “Molecular dynamics simulations of a nucleosome and free DNA,” *J. Biomol. Struct. Dyn.* **22**, 673–685 (2005).
- ¹⁹M. Pasi, K. Zakrzewska, J. H. Maddocks, and R. Lavery, “Analyzing DNA curvature and its impact on the ionic environment: Application to molecular dynamics simulations of minicircles,” *Nucleic Acids Res.* **45**, 4269–4277 (2017).
- ²⁰J. Mongan, “Interactive essential dynamics,” *J. Comput.-Aided Mol. Des.* **18**, 433–436 (2004).
- ²¹F. H. C. Crick and A. Klug, “Kinky helix,” *Nature* **255**, 530–533 (1975).
- ²²K. Rippe, P. H. von Hippel, and J. Langowski, “Action at a distance: DNA-looping and initiation of transcription,” *Trends Biochem. Sci.* **20**, 500–506 (1995).
- ²³J. Pérez-Martín, F. Rojo, and V. de Lorenzo, “Promoters responsive to DNA bending: A common theme in prokaryotic gene expression,” *Microbiol. Rev.* **58**, 268–290 (1994).
- ²⁴G. Sahu, D. Wang, C. B. Chen, V. B. Zhurkin, R. E. Harrington, E. Appella, G. L. Hager, and A. K. Nagaich, “p53 binding to nucleosomal DNA depends on the rotational positioning of DNA response element,” *J. Biol. Chem.* **285**, 1321–1332 (2010).
- ²⁵R. E. Dickerson and T. K. Chiu, “Helix bending as a factor in protein/DNA recognition,” *Biopolymers* **44**, 361–403 (1997).
- ²⁶S. Geggier and A. Vologodskii, “Sequence dependence of DNA bending rigidity,” *Proc. Natl. Acad. Sci. U. S. A.* **107**, 15421–15426 (2010).